# Adiabatic ION Shuttling Protocols in Outer-Segmented-Electrode Surface ION Traps

**Altaf H. Nizamani[1], Bilal Rasool[2], Muhammad Tahir[2,3], Nek M. Shaikh[1], Hussain Saleem[4]**

**Abstract**— Effective and efficient trapped ion transportation operations are important for many quantum information implementations. This paper presents an efficient shuttling protocol for the linear shuttling of ions in asymmetric surface trap geometries in which outer electrode is segmented to provide control over ion transportation from one trapping region to another trapping region. During the adiabatic shuttling operations, the maximum transportation speed of trapped ions depends on the secular frequencies of trapped ions during the process. This paper further express how adiabatic linear shuttling protocols can be implemented in optimised surface trap geometries. In order to make the shuttling process adiabatic, the important parameters that need to be taken into account, are also discussed.

**Index Terms**— Ion shuttling, Ion traps, LASER, Optimum traps, Quantum computation, Quantum information, Surface Trap Geometries.

## 1 Introduction

In the past decade, considerable work has been done towards building the scalable architectures to implement quantum information processing with trapped ions [1],[2],[3]. The focus is on micro-fabricated surface trap arrays where the ions are trapped above the surface of a planar trap structure. In order to have effective quantum operations, it is suggested that if ions can be trapped in separate trapping zones and when quantum operations are required, they can be brought together in a single trapping region i.e. processor zone [4],[5],[6]. Shuttling process has been demonstrated successfully in linear trap arrays and through T and Y-junctions [7],[8],[9]. Home and Steane have discussed and elaborated optimisation of electrode geometries in [10]. Hucul *et. al.* and Reichle *et. al.* have also explained the energy gain of trapped ions during shuttling operations in [11] and [12] respectively. We have combined their useful findings and implemented them to examine the linear ion shuttling process in surface trap arrays. We have also provided a description of how such arrays need to be optimised to have authorization for efficient and adiabatic shuttling. Furthermore, we have provided a detailed analysis of the dynamics of the process by solving the equations of motion and presented a discussion about the considerations that can be taken into account to make the shuttling process adiabatic in outer-segmented geometries. The trap geometries can be categorised in two types: (1) Asymmetric ion traps and (2) Symmetric ion traps. In asymmetric traps, the electrodes lie in a plane and the ions are trapped above that plane, while in symmetric trap designs, the electrodes are symmetrically placed around the position of the trapped ion. Asymmetric traps are known as planar or surface traps and symmetric traps are known as multilayer traps. The main advantage of the planar trap configuration is its ability to be expended to large arrays, in order to construct a quantum computer. In this paper, we have discussed the dynamics of the linear shuttling process in realistic trap arrays. We have also presented a guide to accomplish efficient, adiabatic and fast ion transportation in one-dimension.

## 2 Optimised Surface Trap Geometries

Designing of an optimised basic element of surface trap arrays where ions can be trapped by applying appropriate voltages on the trap electrodes with a maximum trap depth at a given ion-electrode distance is discussed in [13],[14]. In a typical three-dimensional linear RF Paul trap, the RF field provides trapping in the radial axes ($x$ and $y$-directions) whereas a dc-potential provides confinement in the axial direction ($z$-direction). Eq.(1) gives the effective trapping potential in all three directions [11].

$$\Psi(\chi,t) = \frac{q_e^2 V_{RF}^2}{4m\Omega_{RF}^2}|\nabla\theta_{RF}(\chi)|^2 + q_e\sum_n V_n(t)\theta_n(\chi) \quad \cdots(1)$$

Where $m$ and $q_e$ are the mass and charge of the trapped ion. $\chi$ is the position vector. $\theta_{RF}(\chi)$ is the instantaneous electric RF-potential. $\theta_n(\chi)$ is the dc-potential produced by the $n^{th}$ dc-electrode when $V_n$ = 1 V. The peak RF-voltage $V_{RF}$ is applied on the RF-electrodes with drive frequency $\Omega_{RF}$ and the coefficient $V_n(t)$ is the time varying voltage applied on the $n^{th}$ control electrode. A pseudopotential provided by the RF electrodes are represented in the first part of Eq.(1).

Fig.1 elaborate the planer or surface RF trap geometry where
axial confinement is implemented with outer-segmented electrodes, and trapped ion location is illustrated in cross section view of the design.

[1] *Institute of Physics, University of Sindh, Jamshoro, Pakistan*
[2] *Department of Physics, University of Sargodha, Sargodha, Pakistan*
[3] *King Abdullah University of Sc. & Tech., Thuwal, Kingdom of Saudi Arabia*
[4] *Department of Computer Science, University of Karachi, Karachi, Pakistan*

*Email: altaf_nizamani@yahoo.com, hussainsaleem@uok.edu.pk (Corresponding Author)*

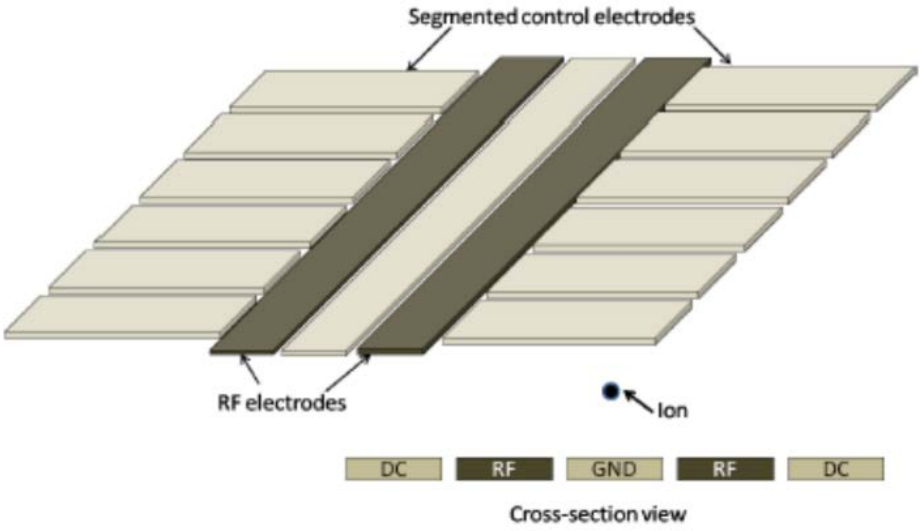


Fig-1: Planer or Surface RF Trap Geometry.

The position of the RF-node or minimum of the pseudopotential where the ions can be trapped is illustrated in Fig.2, where $h$ is the ion–electrode distance (ion-height) above the surface of the trap in the $y$-direction and $x_o$ is the position of the ion in the $x$-direction. The escape point of the ion is located above the trapping position.

The labels $b$ and $c$ in Fig.2 represent widths of the RF-electrodes whereas $a$ is separation between the RF-electrodes. The analytical model suggested by House [13], can be used to calculate the basis functions for the trap electrodes.

The trapped ion(s) can be confined and shuttled in the $z$-direction by applying and varying dc-voltages on the segmented electrodes. In order to reduce the heating of the trapped ion during its shuttling process, the width of a segmented electrode $w$ should be chosen in a way that the trapping field could get a significant curvature everywhere along the transportation path of the ion near the electrode [13]. Therefore, for the trap design shown in Fig.3, outer segmented electrode widths may be chosen as $w=4a$. To avoid diffraction effect of the LASER lights from the trap surface and anomalous heating, ions have to be trapped above the surface electrodes at larger ion-electrode distance but this decreases the trap depth. The optimised trap design suggested in [13],[14] reduces this effect.

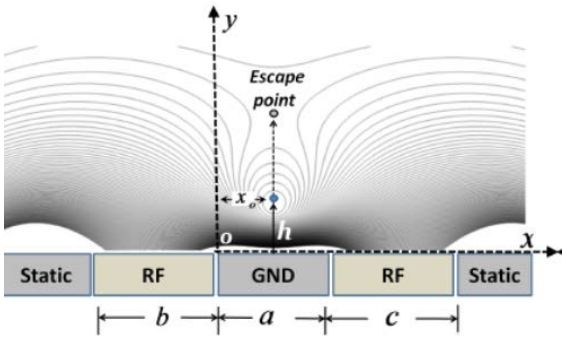


Fig-2: The pseudopotential above the surface trap electrodes.

## 3 Ion Dynamics During Shuttling Process Ion Dynamics

The adiabatic shuttling protocol is described as transportation of the ions in the arbitrary locations within the trap array without significantly manipulating the motional state of the ions. Hucul et al. [11] and Reichle et al. [12] have shown the importance of shuttling protocols using functions. Hucul et al. described the advantages of the hyperbolic tangent profile $P_{hyp}(t)$ by Eq.(2).

$$P_{hyp}(t) = tanh\left[N \times \left(\frac{t-T}{T}\right)\right] \qquad \cdots (2)$$

In Eq.(2), $T$ is the total shuttling time whereas $t$ is the instantaneous shuttling time. The larger values of $N$ produce more gradual changes for values of $t$ near to zero (0) and $T$, while incorporating larger rates of change for values of $t$ near to $\frac{T}{2}$. By using the basis functions for individual electrodes, an arbitrary time dependent potential can be created.

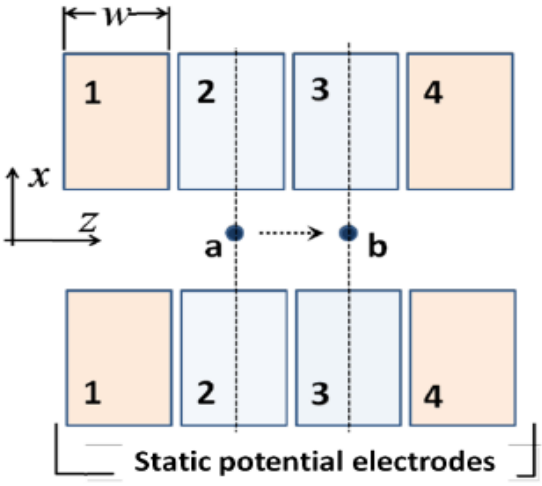


Fig-3: Trapping zone 'a' to 'b' in z-direction.

The classical equations of motion can be utilized to

calculate the force on a charged particle [11]; is described by Eq.(3).

$$\sum_{n}^{3} m\chi_n + \nabla_n \psi(\chi_j, t) = 0 \qquad \cdots (3)$$

The pseudopotential $\psi(\chi_j, t)$ is early defined in Eq.(1). However the ion trajectories can be calculated by solving Eq.(3) numerically. The ion dynamics in the *x*, *y* and *z* directions as a function of time $t$ can be calculated by getting highly accurate solutions of Eq.(3). The solutions can also be used to calculate the kinetic energy gained by the ion. In order to solve these differential equations, we have used a Mathematica-7 Software package called "NDSolve" and obtained fine and accurate results.

### 3.1 Average Motional Energy

In a quantum harmonic oscillator of frequency $\omega_0$, the average energy $\langle E \rangle$ of level $\langle n \rangle$ is given by Eq.(4).

$$\langle E \rangle = \hbar\omega \left( \langle n \rangle + \frac{1}{2} \right) \qquad \ldots (4)$$

$$\langle n \rangle_s = \frac{\frac{1}{2} m v_t^2}{\hbar \omega_t} \qquad \ldots (5)$$

The average motional quanta $\langle n \rangle$ for a trapped ion can be calculated using Eq.(5). Where $v_t$ is the maximum velocity, $m$ is the mass of the ion and $\omega_t$ is the instantaneous secular frequency. In the frame of the pseudopotential well, the kinetic energy of the ion is only due to its secular motion. The maximum kinetic energy of the ion at the beginning and end of the shuttling process can be obtained by plotting the kinetic energy of the ion as a function of the shuttling time. Therefore, the average change of motional state of the shuttled ion is determined through Eq.(6). Where, $(K.E.)_{max}$ is the maximum Kinetic Energy of the ion in a potential well.

$$\langle n \rangle_s = \frac{(Final\ K.E.)_{max} - (Initial\ K.E.)_{max}}{\hbar \omega_t} \qquad \cdots (6)$$

### 3.2 Motional Heating caused by Anomalous Heating

The motional excitation of an ion during shuttling process can be caused by anomalous heating due to small ion-electrode distance in the trap. It is experimentally shown that the heating rate $\langle \dot{n} \rangle_{an}$ is related to the ion-electrode distance and scaled to $h^4$ and to the secular frequency scaling as $\omega^2$ [15]. A conservative approximation of the motional state excitation of the $Yb^+$ (Ytterbium) due to anomalous heating is carried out by [15] provided a realistic estimate in Eq.(7).

$$\langle \dot{n} \rangle_{an} \approx \frac{1.97 \pm 0.5 \times 10^{26} \mu m^4 Hz^3}{\omega^2 h^4} \qquad \cdots (7)$$

Where $\omega$ is in units of $s^{-1}$ and $h$ is ion–electrode distance in units of micrometres (μm). This expression is only valid for the particular ion trap and ion specie for which it was intended to measure. However it still provide a reasonable estimate of heating rate for illustration purposes. Note that the optimisation of electrode surfaces and materials can substantially reduce heating rate. During the shuttling process, the motional quanta $\langle n \rangle_{an}$ obtained from the anomalous heating, can be calculated through Eq.(8) by integrating $\langle \dot{n} \rangle_{an}$ over the shuttling time $t$ [14].

$$\langle n \rangle_{an} = \int_{t_o}^{t_f} \langle \dot{n} \rangle_{an}\, dt \qquad \cdots (8)$$

Where, $t_o$ and $t_f$ are the beginning and the ending time for a shuttling process. The integral in Eq.(8) also takes into account the changing secular frequencies $\omega_z$ during the shuttling process [14]. Hence, the total number of the motional quanta $\langle n \rangle$ can be calculated by Eq.(9).

$$\langle n \rangle = \langle n \rangle_s + \langle n \rangle_{an} \qquad \cdots (9)$$

In order to demonstrate the importance of optimal trap geometries for ion transportation, it is useful to analyse the actual ion dynamics during the shuttling process. We have obtained actual simulations for a given set of example parameters. The conclusions obtained in this section are applicable for a wide range of trap geometries featuring different ion-electrode distances.

The optimisation of the trap electrodes for the maximum κ and β parameters are also investigated. These two important parameters provide maximum trap depth and secular frequency during the shuttling process. A set of actual values of κ and β are needed to carry out simulations of the ion dynamics during shuttling process. For this, we need a realistic set of electrode voltages that can be applied to the trap. The trap depth σ and the RF trap stability factor $q$ are related as described in Eq.(10) and Eq.(11) respectively.

$$\sigma = \frac{V_{RF}}{2\pi^2} \kappa q \qquad \cdots (10)$$

$$q = \frac{2 q_e V_{RF}}{m \Omega_{RF}^2 h^2} \qquad \cdots (11)$$

Limited set of voltages can be applied on microfabricated ion traps due to voltage breakdown via insulator bulk and surfaces. Therefore, in order to achieve a deep trap, one should choose $q$ as large as possible without getting out of the region of stability in parameter space. Therefore, the value of $q$, near to 0.7 seems a reasonable choice. Another important parameter to be considered is the power dissipation within the ion trap which can lead to destruction of the chip. The Power dissipation $P_d$ of a trap having capacitance $C$ and resistance $R$, can be estimated using Eq.(12). The method is also explained in [16],[17].

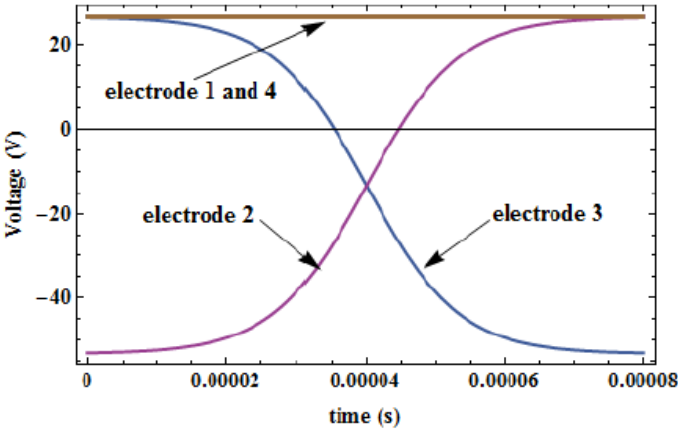


Fig-4: The voltage variation in time to move the trapped ion from the trapping zone 'a' to 'b'. The hyperbolic tangent time profile is used.

$$P_d \approx 0.5 V_{RF}^2 \Omega_{RF}^2 C^2 R \qquad \cdots (12)$$

It is worthmentioned that an approximate $P_d \approx 3\ Watts$ power normally do not lead to a large temperature change in typical ion trap chips. We have considered a typical microfabricated chip having electrodes made-up of electroplated gold on a commercially available Silicon Oxide ($SiO_2$) insulator wafer according to the technique mentioned in [18]. The thickness of the electrodes is considered to be ≈ 15 μm. In such traps, we can estimate typical values of $R \approx 0.5\Omega$ and $C \approx 20$pF for the resistance and capacitance respectively. Assuming $\Omega_{RF} \approx 2\pi \times 55MHz$ for the above trap, one could safely apply $V_{RF}$ of approx. 460−500 Volts by setting $q \approx 0.7$. These values are estimated to trap $_{171}Yb^+$ ion. The power dissipation for this trap can be calculated as $P_d < 3\ Watts$. In order to avoid damaging the chip, we limit voltage difference between adjacent electrodes near to 500Volts [19].

In order to feature adequately low motional excitation due to anomalous heating during the shuttling, we take sufficiently large ion-electrode distance. For this reason, we have selected here an ion-electrode distance of ≈ 80μm. For an example, a trap depth of ≈ 0.35eV and radial secular frequencies ($\omega_x$ and $\omega_y$) of up to ≈ 4.4MHz for an $_{171}Yb^+$ ion can easily be achieved in the trap by using the trap parameters mentioned above. Once the ion-electrode distance above the surface is chosen, all other electrode dimensions are determined accordingly. For principal axis rotation, assuming un-equal RF electrodes $b = \frac{c}{2}$ optimum widths are therefore $b \approx 300$μm and $c \approx 150$μm. The electrodes can be separated by a ground electrode of width 50μm (i.e. the separation between RF electrodes is $a = 60$μm including 5μm gap between RF-electrodes and the ground electrode). The optimum widths for the control electrodes for the design shown in Fig.3, are then to be W = C = E ≈ 220μm as discussed earlier. For an exemplary trap geometry, we also refer to an outer segmented design shown in Fig.3 for which the constraints and dimensions are explained above. In order to calculate the overall motional excitation, we have solved the equations of motion for the shuttled ion. We believe that the conclusion results obtained for the particular trap parameters stated above, is highly applicable for many surface trap arrays.

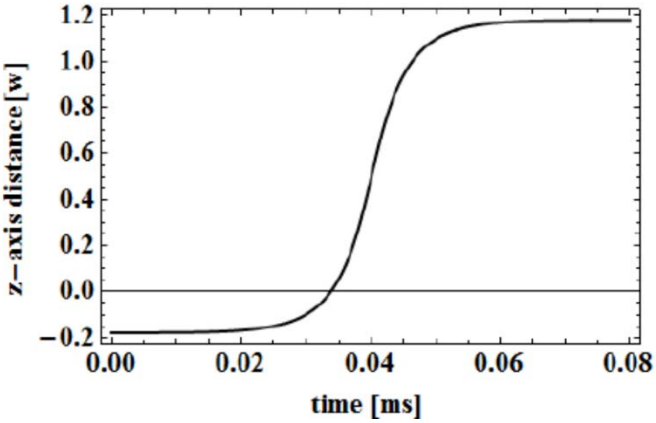


Fig-5: The distance shuttled by the ion when the dc voltage change with a hyperbolic tangent time profile is applied. The shuttled distance in
z-direction is normalised with the width of the electrode.

### 3.3 Ion Shuttling in the Outer Segmented Trap

In the case of outer-segmented trap geometries discussed above, an ion can be confined in the z-direction by using at least 6 control electrodes. Therefore, to produce two adjacent trapping zones along the RF nodal path (axial direction), it requires minimum 8 control electrodes. The trapping zones 'a' and 'b' in such geometries are shown in Fig.3. Here the radial confinement is provided by RF electrodes (RF electrodes are not shown in the figure). To ensure symmetry in the radial direction, opposite facing control electrodes are connected to the same voltage supply. The RF voltage is set to $V_{RF} = 450V$ with a driving frequency of $\Omega_{RF} = 2\pi \times 52MHz$ and dc-voltages are limited to ±50 V. By applying the above voltages, the secular frequencies in $x$ and $y$ directions can be calculated as $\omega_x \approx \omega_x \approx 4MHz$ and the trap depth is ≈ 0.35eV.

The basis functions for the control electrodes can be calculated using analytical method suggested by House [13]. All the other required parameters of the trap ion can be calculated using Mathematica Software. The voltages on the endcap control electrodes (1 and 3) for trapping zone 'a' are first set to some arbitrary value and then the required voltage on electrode 2 is calculated to keep the ion at the RF node position. In the second stage, all the voltages are scaled iteratively until a desired value of a secular frequency $\frac{\omega_0}{2\pi}$ in the z-direction is obtained. The same calculation process is repeated to obtain a set of voltages for the trapping zone 'b'. In an optimum trap geometry shown in Fig.3, to see the effect of N-parameters of hyperbolic tangent time profile (discussed above) with different shuttling times, the ramping profile of the voltages (shown in Fig.4) are applied with N-parameter of N = (2.6, 3.0, 3.4) values to shuttle an ion from zone 'a' to 'b'. At the start of the shuttling protocol, electrodes 1, 3 and 4 are held at +26V and electrode 2 initially at -50V. The secular frequency $\omega_0$ in the z-direction in trapping zone 'a' is calculated to be approximately ≈ 500kHz. In order to move the ion from zone

'a' to zone 'b', the voltage on electrode 2 has to be brought to +26V and the voltage on electrode 3 has to be brought to -50V, monotonically in time $t$.

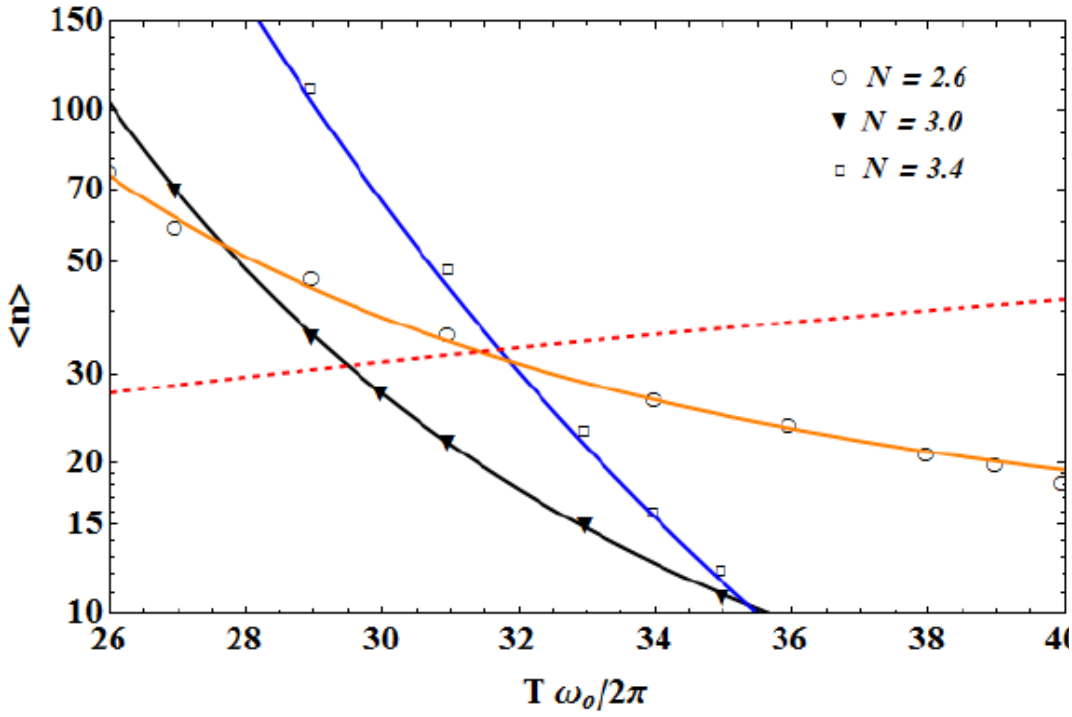


Fig-6: The gain in the average motional quanta ⟨n⟩ by the ion in a centre segmented trap geometry after the shuttling of the ion from trapping zone 'a' to 'b' following the hyperbolic tangent time profile of N = (2.6, 3.0, 3.4) versus shuttling time scaled with secular frequency $\omega_o/2\pi$ = 500 kHz. The solid lines represent the best fits of motional quanta $\langle n \rangle_s$ and the dashed line shows the gain of $\langle n \rangle_{an}$ from the anomalous heating of the trap. The cross over points set lower limits for the gain in ⟨n⟩ during the shuttling process.

The ion will be moved to trapping zone 'b' from initial trapping zone 'a' after the completion of the voltage ramps. The secular frequency remains the same in both trapping zones. By following the voltage ramp profile given in Fig.4, the ion is successfully shuttled a distance of ≈ 225μm from zone 'a' to 'b'. A typical ion trajectory in the z-direction is shown in Fig.5 when the dc-voltage change with the hyperbolic tangent time profile is applied. The average motional quanta $\langle n \rangle$ are plotted against the shuttling periods which are scaled with the secular frequency $\omega_0$ and represented in number of cycles $T\frac{\omega_0}{2\pi}$ in the horizontal axis in Fig.6. Here, it can be learnt from the plots that the gain of the average motional quanta $\langle n \rangle_s$ of the ion is reduced with larger shuttling time but on the other side, the longer shuttling periods add more quanta from the anomalous heating source. Hence the cross over points for $\langle n \rangle_s$ gained by following the particular hyperbolic tangent N-parameter plots (solid lines) and the $\langle n \rangle_{an}$ (dashed line) set the lower limit of the total average motional quanta $\langle n \rangle$ gained by the ion during the shuttling. Further to this, it can be seen in Fig.6 that the hyperbolic tangent parameter N = 3.0 adds less quanta at the cross over point than the N = 2.6 or N = 3.4 and also provides shorter shuttling times [20].

## 4. CONCLUSION

Using realistic trap geometry in our considerations, we have learned a lot about optimal trap designs by analysing the actual dynamics of the ion transportation process. Given that the presence of anomalous heating in the traps caused by fluctuating and stray charges on the trap electrodes, the conclusion from our results show that optimal geometries should be pre-requisite to ensure adiabatic shuttling. We have demonstrated the role of optimum trap geometries for efficient fast ion shuttling in scalable surface ion traps. It is known that, a shuttling process adds less energy to the ions if performed under higher secular frequencies. By optimisation of the electrode dimensions, the secular frequencies $\omega_z$ during the shuttling process can be maximised. The secular frequency depends upon two important trap parameters κ and β. By analysing a realistic microfabricated trap design, we have solved the equations of motion for the dynamics of ion shuttling and illustrated the importance of optimised electrode configurations in outer segmented trap geometries. The outer segmented design can be a geometry of choice due to the much simpler fabrication process.

## REFERENCES

[1] J. I. Cirac & P. Zoller, "Quantum Computations with Cold Trapped Ions", *Phys. Rev. Lett. 74*, 4091, (1995)
[2] C. Monroe, "Quantum Information Processing with Atoms and Photons", *Nature 416*, 238, (2002)
[3] H. Haffner, C. F. Roos, & R. Blatt, "Ion Trap Quantum Computing with $Ca^+$ Ions", *Physics Reports 469*, 155, (2008)
[4] D. J. Wineland, C. Monroe, W. M. Itano, D. Leibfried, B.E. King, & D.M. Meekhof, "Experimental Issues in Coherent Quantum-State Manipulation of Trapped Atomic Ions", *J. Res. Natl. Inst. Stand. Technol, 103*, 259, (1998)
[5] J. I. Cirac & P. Zoller, "A Scalable Quantum Computer with Ions in An Array of Microtraps", *Nature, 404*, 579, (2000)
[6] D. Kielpinski, C. Monroe, & D. J. Wineland, "Architecture for a Large Scale Ion-Trap Quantum Computer", *Nature, 417*, 709, (2002)
[7] W. K. Hensinger, S. Olmschenk, D. Stick, D. Hucul, M. Yeo M. Acton, L. Deslauriers, C. Monroe, & J. Rabchuk, "T-Junction Ion Trap Array for Two-Dimensional Ion Shuttling, Storage, and Manipulation", *Appl Phys. Lett., 88*, 034101, (2006)
[8] S. Schulz, U. Poschinger, K. Singer, & F. Schmidt-Kaler, "Optimization of Segmented Linear Paul Traps and Transport of Stored Particles", *Fortschr. Phys., 54*, 648, (2006)
[9] J. M. Amini *et. al.*, "Toward Scalable Ion Traps for Quantum Information Processing", *New Journal of Physics, 12*, 033031, (2010)
[10] J. P. Home & A.M. Steane, "Electrode Configurations for Fast Separation of Trapped Ions", *Quant. Inf. Comp., 6*, 289, (2006)
[11] D. Hucul, M. Yeo, W. K. Hensinger, J. Rabchuk, S. Olmschenk & C. Monroe, "On the Transport of Atomic Ions in Linear and Multidimensional Ion Trap Arrays", *Quant. Inf. Comp., 8*, 0501, (2008)
[12] R. Reichle, *et. al.*, "Transport Dynamics of Single Ions in Segmented Microstructured Paul Trap Arrays", *Phys., 54*, 666, (2006)
[13] M. G. House, "Analytic Model for Electrostatic Fields in Surface Electrode Ion Traps", *Phys. Rev. A, 78*, 033402, (2008)
[14] Altaf H. Nizamani, & Winfried K. Hensinger, "Optimum Electrode Configurations for Fast Ion Separation in Microfabricated Surface Ion Traps", *Applied Physics B, 106*, 2, (2012)
[15] L. Deslauriers, S. Olmschenk, D. Stick, W. K. Hensinger J. Sterk, & C. Monroe, "Scaling and Suppression of Anomalous Heating in Ion Traps", *Phys. Rev. Lett., 97*, 103007, (2006)
[16] James J. McLoughlin, Altaf H. Nizamani, James D. Siverns Robin C. Sterling, *et.al.*, "Versatile Ytterbium Ion Trap Experiment for Operation of Scalable Ion-Trap Chips with Motional Heating And Transition Frequency Measurements", *Phys. Rev. A, 83* , 013406, (2011)
[17] M. D. Hughes, B. Lekitsch, J. A. Broersma, & W. K Hensinger, "Microfabricated Ion Traps", *arXiv:1101.3207v2*, (2011)
[18] S. Seidelin, *et. al.*, "Microfabricated Surface-Electrode Ion Trap for Scalable Quantum Information Processing", *Phys. Rev. Lett., 96*, 253003, (2006)
[19] Altaf H. Nizamani, M.A. Rind, Nek M. Shaikh, A. H. Moghal & Hussain Saleem, "Versatile Ultra High Vacuum System for ION Trap Experiments: Design and Implementation", *Intl. Journal of Advancements in Research & Technology, USA*, Vol.2, Issue.5, (2013)
[20] S.A. Buzdar, M. Afzal Khan, Aalia Nazir, M.A. Gadhi, Altaf H. Nizamani & Hussain Saleem, "Effect of Change in Orientation of Enhanced Dynamic Wedges on Radiotherapy Treatment Dose", *Intl. Journal of Advancements in Research & Technology, USA*, Vol.2, Issue.5, (2013)

**Altaf Hussain Nizamani** is working as Assistant Professor at the Institute of Physics, University of Sindh, Jamshoro, Pakistan. He received Ph.D degree in Ion-Trapping and Quantum computation technology from the University of Sussex, Brighton, UK in 2011. His areas of interests are Scalable Ion trap chips for the quantum computing and information technology, ultra high vacuum system designing, FPGA and Real-time LabVIEW programming, LASER cooling & trapping and computational Physics.

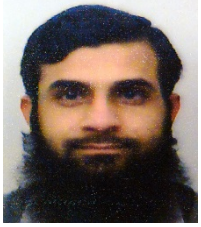

**Bilal Rasool** is an Assistant Professor in the Department of Physics, at University of Sargodha, Pakistan. He has completed his Ph.D in Surface Science/Ion Plasma, from University of Innsbruck, Austria. His area of interests are Surface Sciences, Condensed Matter Physics, Plasma Physics, Ion Implantation and LASER induced Plasma Physics.

**Muhammad Tahir** Is a Postdoc Fellow at Physical Science & Engineering (PSE) Department, King Abdullah University of Science & Technology (KAUST), Kingdom of Saudi Arabia. He was awarded Ph.D. degree in Theoretical Condensed Matter Physics from Imperial College London, U.K., in 2010. He has completed his M.Phil in Theoretical Condensed Matter Physics from Quaid-e-Azam University, Islamabad, Pakistan, in 2004. He is working in Quantum Transport and Collective Excitations Spectrum including Static and Dynamic dielectric response of 2-Dimensional systems like Graphene, Silicene, and Topological Insulators. He has published more than 24 papers in international journals.

**Nek Muhammad Shaikh** is an Associate Professor at the Institute of Physics, University of Sindh, Jamshoro. He has completed his Ph.D. in LASER Spectroscopy, from the Atomic and Molecular Physics Laboratory, Department of Physics, Quaid-e-Azam University, Islamabad, Pakistan. He has also completed his Post-Doctorate from the Center for Energy Research, University of California, San Diego, California, USA, in 2009, where he worked on the different experimental techniques to increase conversion efficiency of the Extreme Ultraviolet (EUV) light using LASERs. His area of interests are LASER-Induced Breakdown Spectroscopy, LASER Spectroscopy and LASER Physics.

**Hussain Saleem** is Assistant Professor and Ph.D. Research Scholar at Department of Computer Science, University of Karachi, Pakistan. He received B.S. in Electronics Engineering from Sir Syed University of Engineering & Technology, Karachi in 1997 and has done Masters in Computer Science from University of Karachi in 2001. He also received Diploma in Statistics from University of Karachi in 2007. He bears vast experience of more than 16 years of University Teaching, Administration and Research in various dimensions of Computer Science. Hussain is the Senior Instructor and has been associated with the Physics Labs at Aga Khan Ex. Students Association Karachi since 1992. He served as Bio-Medical Engineer at Aga Khan University in 1999-2000, where he practiced to handle Radiology, LASERs, and MRI equipments. Hussain is the Author of several International Journal publications. His field of interest is Software

Science, System Automation, Hardware Design & Engineering, Data Analysis, and Simulation & Modeling. He is senior member of Pakistan Engineering Council (PEC).